

DEEP NEURAL NETWORKS FOR RADAR WAVEFORM CLASSIFICATION

Michael Wharton[†], Anne M. Pavy[‡], and Philip Schniter^{}*

^{†‡}Sensors Directorate, Air Force Research Lab, WPAFB, OH, 45433, {michael.wharton.3, anne.pavy}@us.af.mil

^{*}Dept. ECE, The Ohio State Univ., Columbus, OH, 43210, schniter.1@osu.edu

ABSTRACT

We consider the problem of classifying radar pulses given raw I/Q waveforms in the presence of noise and absence of synchronization. We also consider the problem of classifying multiple superimposed radar pulses. For both, we design deep neural networks (DNNs) that are robust to synchronization, pulse width, and SNR. Our designs yield more than 100x reduction in error-rate over the current state-of-the-art.

1. INTRODUCTION

We consider the problem of classifying radar waveforms given as raw complex-valued time sequences. Waveform classification plays an important role in cognitive radar [1, 2] and other applications. For classifier design, we assume the availability of a dataset containing many examples of radar waveforms (i.e., sequences of complex-valued time-domain samples) with corresponding class labels in $\{1, \dots, K\}$; we do not assume any physical model. In this work, we focus on deep neural network (DNN) classifiers, as they have shown to be state-of-the-art in many related tasks.

The radar application imposes several unique challenges on DNN classifier design. First, radar pulse widths can span a very wide range (e.g., several orders-of-magnitude), even within a given class. Second, radar pulses cannot be assumed to be time-synchronized in the observation window. Third, practical radar systems must operate over a huge range of signal-to-noise ratios (SNRs), including SNRs far below 0 dB. Fourth, the pulses are complex-valued, whereas most DNNs are designed for real-valued signals. All of these challenges make the classification of radar pulses quite different from typical classification problems to which DNNs are applied (e.g., image classification).

Early approaches to radar waveform classification first converted the raw waveforms to hand-crafted, low-dimensional features, to which classic machine-learning techniques could be applied. For example, [3] designed auto-correlation function (ACF) features of dimension 20 that were robust to time and frequency shifts, and trained a Fisher’s linear discriminant classifier. These ACF features were later used in [4] with

a support vector machine (SVM) classifier and in [5] with a shallow neural-network classifier.

It was recently demonstrated in [5] that significantly better classification accuracy could be obtained by training a DNN to operate on raw time-domain radar waveforms in place of ACF features. This is not surprising, since DNNs are able to learn features that outperform hand-crafted ones.

Still, several assumptions were made in [5] that limited both the performance and practicality of their design. First, the DNN input dimension in [5] was chosen to be greater than the longest pulse in the training dataset. We will show that it is better to truncate or pad the pulses to an optimized input length. Second, the DNN in [5] ignored the quadrature (Q) input to avoid complex-valued operations. We show that a well-designed complex-valued DNN has advantages over a real-valued DNN in this application. Third, the training and test waveforms in [5] were assumed to be time-synchronized, which is impractical. We train our DNN to be robust to time-asynchronous inputs. Fourth, the DNN architecture in [5] can be significantly improved, as we show. Additionally, the training procedure can be improved via the use of data augmentation (i.e., random noise and delay realizations). Fifth, [5] assumed a single radar pulse, whereas we propose a DNN-based approach to multi-pulse radar waveform classification, which—to our knowledge—is the first in the literature.

2. APPROACH

2.1. Network Architecture

Like in [5], we focus on feed-forward convolutional DNNs. (Although we also experimented with recursive networks, we did not find the results to be competitive.) We evaluated 1D residual networks (ResNets) [6], ResNeXts [7], and DenseNets [8] due to their excellent performance on generic classification tasks. As we will discuss later, we found that the ResNet worked best for our data.

2.2. Complex Arithmetic

Many approaches have been proposed to handle complex-valued signals with real-valued DNNs, however success depends largely on the application. Feeding the magnitude of

[†]Supported in part by NSF Grant 1539961

the complex-valued signal to the DNN successfully classified synthetic aperture radar images in [9], but we found this to work poorly with our radar data. Another approach is to feed only the real part of the complex-valued signal to the DNN. Although this was used in [5], we show in the sequel that it can be improved upon. Another approach is to stack the real and imaginary parts of the waveform into a real-valued 2-row “image” and feed it to a real-valued DNN with 2-dimensional convolutions [10]. Yet another approach is to feed the real and imaginary parts into two input channels of a real-valued DNN.

An alternative is to design a complex-valued DNN. Such networks have led to improved performance in, e.g., audio classification [11] and magnetic resonance image (MRI) reconstruction [12] tasks. To understand what we mean by a “complex-valued DNN,” consider the multiplication of a learnable parameter $k = k_r + ik_i \in \mathbb{C}$ with a feature $x = x_r + ix_i \in \mathbb{C}$, where $k_r, x_r \in \mathbb{R}$ represent real parts, $k_i, x_i \in \mathbb{R}$ represent imaginary parts, and $i \triangleq \sqrt{-1}$. Such multiplications arise in the convolutional layers of DNNs. The complex-valued multiplication of k and x can be written using four real-valued multiplications as

$$kx = (k_r x_r - k_i x_i) + i(k_i x_r + k_r x_i). \quad (1)$$

The key point is that (1) is a two-input/two-output operation with only two learnable parameters: $k_r, k_i \in \mathbb{R}$. By contrast, a 2-channel real-valued DNN would implement

$$\begin{aligned} y_1 &= k_{11}x_1 + k_{12}x_2 \\ y_2 &= k_{21}x_1 + k_{22}x_2, \end{aligned} \quad (2)$$

with $x_1 \triangleq x_r$ and $x_2 \triangleq x_i$, which involves four learnable parameters: $k_{11}, k_{12}, k_{21}, k_{22} \in \mathbb{R}$. By reducing the number of learnable parameters, we can reduce overfitting.

With regards to complex-valued activation functions, both [11, 12] suggest that separately applying the ReLU function to the real and imaginary parts outperforms other complex-valued activations in many applications, so we use this approach in our networks.

Complex-valued implementations of batch-norm have also been developed (see, e.g., [12]). For simplicity, we apply standard batch-norm separately to real and imaginary parts.

2.3. Noise Padding / Truncation / Delay

As mentioned earlier, our raw radar waveforms differ in duration from hundreds to thousands of samples. But DNNs force us to choose a fixed input dimension for minibatch training. The usual approach would be to set the input dimension equal to the longest sample and zero-pad the others as needed.

With noisy radar waveforms, however, it is more appropriate to noise-pad than to zero-pad, since in practice the test waveforms will be noise padded. Thus, in [5], the waveforms were symmetrically padded with white Gaussian noise whose

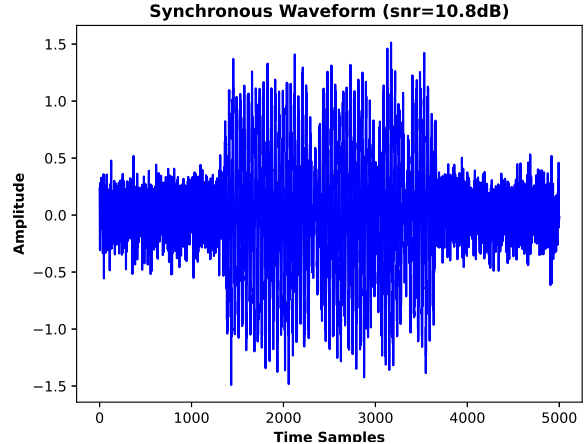


Fig. 1. Example synchronous noise-padded waveform at SNR=10.8dB, $N = 2261$, and $D = 5000$.

variance was chosen to match the noise variance in the original sample. An example is shown in Fig. 1.

There are several issues with the approach from [5]. First, as a consequence of symmetric padding, the padded waveforms will all be time-centered, i.e., synchronized. But since time synchronization is not expected in practice, it is not advantageous to train on time-synchronized waveforms. Second, noise-padding reduces SNR. In particular, if a sample is $P \times$ longer after noise-padding, then its SNR will change by the factor $1/P$. Third, [5] padded each training sample with a *fixed* noise waveform. As a result, the DNN might overfit to this particular noise realization. This latter problem is exacerbated by the very low SNRs encountered in radar.

Our approach is to noise-pad *or* truncate the training waveforms as needed to obtain a fixed input length of D , where D is optimized. To simulate asynchronous pulses, we randomly delay the pulse before noise-padding or truncating. We can describe this precisely using N to denote pulse width and U to denote a random integer uniformly distributed from 0 and $|N - D|$. When $N < D$, we noise-pad the front of the pulse using U samples and noise-pad the back of the pulse using $D - N - U$ samples. (See Fig. 2.) When $N > D$, we keep D consecutive samples of the pulse starting at index U . To avoid (over)fitting the DNN to particular training noise waveforms or delays, we draw new realizations of these quantities in every training minibatch (e.g., in the DataLoader of PyTorch [13]). This approach can be considered is a form of “data augmentation” [14] that effectively increases the number of the training samples.

3. EXPERIMENTAL RESULTS

For our experiments, we use the SIDLE dataset, which was also used in [3–5]. This dataset contains 23 classes of phase-modulated radar pulses with 10000 examples of single pulses

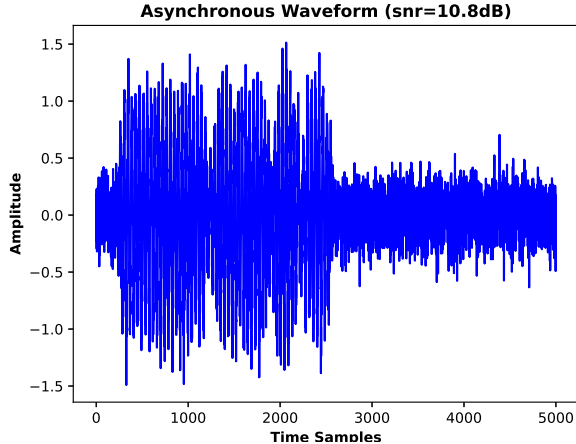


Fig. 2. Example asynchronous noise-padded waveform at SNR=10.8dB, $N = 2261$, $D = 5000$, $U = 200$.

from each class. (Please see [3–5] for more details on the dataset.) For a fair comparison to [5], we omitted classes 6 and 19–23 in the original dataset and used only the remaining $K = 17$ classes to train and test our DNN. For these 17 classes, the dataset contains complex-valued waveforms with SNRs uniformly distributed between -12 and $+12$ dB. The modulation types and range of pulse widths are detailed in [5]. For each experiment, we used a random subset of 80% of the dataset for training and the remaining 20% for testing. In what follows, we discuss classification of single pulses in Sections 3.1 and 3.2 and multiple pulses in Section 3.3.

3.1. Baseline

As a baseline, we first investigate the performance of the 9-layer real-valued DNN from [5] on the task of single-pulse classification. As described earlier, this network uses an input dimension of 11000 and discards the imaginary part of the input. To train and test the network, we used the synchronous noise-padding approach from Section 2.3 and illustrated in Fig. 1, and saw that the network converged to 0% training error and 3.57% test error, similar to what was reported in [5].

Next, to evaluate how well this DNN performs in the practical asynchronous setting, we re-trained it using the asynchronous noise-padding approach proposed in Section 2.3 and illustrated in Fig. 2. When testing with asynchronous data, we observed a test error of 18.29%. This relatively poor performance motivates the design of an improved DNN for asynchronous single-pulse classification.

3.2. Improvements

Architecture: As a first step, we evaluated the ResNet, ResNeXt, and DenseNet architectures, which have more convolutional layers and fewer dense layers than the baseline DNN in [5]. We configured each DNN using PyTorch’s de-

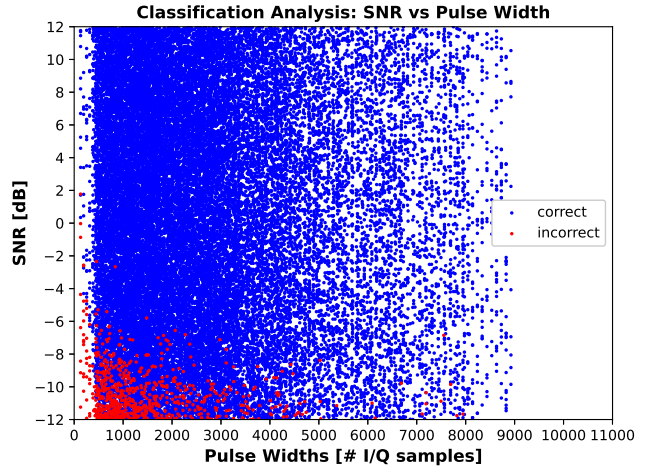


Fig. 3. Classification outcome (true=blue, false=red) of 11000-input ResNet-30 vs. pre-padded SNR and pulse length.

fault parameters, but used 1D convolution. We trained and tested each network with the asynchronous noise-padding approach from Section 2.3, and put the real and imaginary parts into two input channels, which we will show is superior to using just the real part. The ResNet, ResNeXt, and DenseNet achieved test errors of 1.6%, 10.5%, and 2.8%, respectively. Thus, further experimentation focused on the ResNet.

ResNet: For fair comparison to the baseline DNN, we trained a 30-layer ResNet, but we used an input dimension of 11000 and only the real part of the waveform. Training and testing this ResNet-30 using the asynchronous noise-padding approach from Section 2.3 gave 2.14% test error, which significantly improves upon the 9-layer DNN from [5].

Optimized input-length: To better understand how we might be able to improve the ResNet performance, we plot the classification outcome versus pre-padded pulse width and SNR in Fig. 3. The plot shows that pulses with both short length and low SNR are most likely to be misclassified. This is consistent with the discussion in Section 2.3, which described how noise-padding by factor P changes the SNR by factor $1/P$.

To alleviate this problem, we considered reducing the network input dimension D by either truncating or noise-padding each N -length raw waveform as needed. Table 1 reports test error rate for several values of D . The table shows that $D = 3317$ was best among the tested values for the ResNet-30. As a consequence of this D -optimization, the test error improved from 2.14% to 1.32%.

Complex-valued DNN: To improve the DNN further, we incorporate the complex-valued operations from Section 2.2 in the ResNet and refer to it as the “CResNet.” We also considered the 2-channel real-valued DNN from (3), which we call the “IQ-ResNet.” For a fair comparison, we adjusted the number of channels in the CResNet-30 and the IQ-ResNet-30 so that the number of trainable parameters is approximately

Table 1. ResNet-30 vs. Input Length

Input Length	1000	1821	3317	6040	11000
Test Error	8.50%	2.16%	1.32%	1.35%	2.14%

Table 2. ResNet-30 vs. CResNet-30

Model	Test Error	Trainable Parameters
ResNet-30	1.52%	1782193
IQ-ResNet-30	0.39%	1782417
CResNet-30	0.36%	1690189

Table 3. Fine-tuned CResNet Results vs. Network Depth

Model	Test Error	# Parameters	Width	Kernel
CResNet-22	0.16%	7721041	32	11
CResNet-26	0.16%	1818161	16	7
CResNet-30	0.14%	659233	8	9
CResNet-34	0.15%	670945	8	9
CResNet-38	0.16%	2228913	16	7

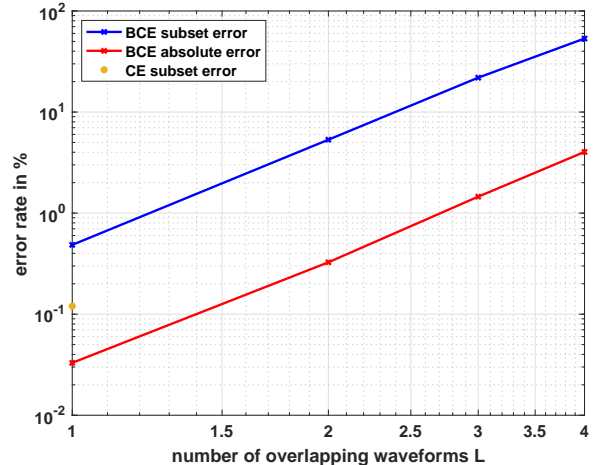
equal to that in the (real-valued) ResNet-30. For all networks we report the number of real-valued trainable parameters (e.g., a complex-valued kernel of length M has $2M$ trainable parameters). The resulting test error rates are shown in Table 2 for $D = 3317$, which shows the improvement brought by the CResNet.

Network Fine-Tuning: As a final step, we performed an extensive fine-tuning of the CResNet. This included a simultaneous search over network depth, network width, kernel width, batch size, and learning rate. For network and kernel width, we adjusted the 1st and 2nd layers respectively, and scaled the remaining layers in the same way as done in the default ResNets in PyTorch. The test error (averaged over 100 random delays and noise realizations) and optimized network parameters of the fine-tuned CResNet are given in Table 3. A batch size of 512, learning rate of 0.001, and first-layer kernel width of 11 sufficed for all widths and depths. Each network was trained for 90 epochs, with early stopping if the test loss did not improve for 15 consecutive epochs. In the end, with fine-tuning, the test error rate dropped to 0.14%.

3.3. Classification of multiple overlapping pulses

We now shift our focus to multi-pulse classification. There, one observes a noisy superposition of L shifted and scaled radar pulses and the goal is to determine whether a pulse is present or absent from each of the K known classes.

To tackle this task, we simply retrained our fine-tuned CResNet to minimize binary cross-entropy (BCE) loss on each of the $K = 17$ outputs, rather than cross-entropy (CE) loss. The resulting network outputs a real-valued logits vector, for which a positive entry in the k th location indicates that a pulse from the k th class is believed to be present, while a negative entry indicates that no pulse is believed to be present.

**Fig. 4.** Subset and absolute error-rate versus L for the BCE-trained and CE-trained networks.

There are two common ways to define the error-rate in multi-label classification: “absolute error” (E_{abs}) refers to the error on the binary predictions, whereas “subset error” (E_{sub}) refers to the error on the K -ary prediction vector as a whole. For i.i.d. binary errors, $E_{\text{sub}} = 1 - (1 - E_{\text{abs}})^K \approx KE_{\text{abs}}$ using the binomial approximation, which is accurate for small E_{abs} .

Our test error-rates for fixed $L \in \{1, 2, 3, 4\}$ are presented in Fig. 4. There we see that both $\log E_{\text{abs}}$ and $\log E_{\text{sub}}$ grow approximately linearly with $\log L$. We also see that $E_{\text{sub}} \approx KE_{\text{abs}}$. Furthermore, we see that the single-pulse network (from Section 3.2) outperformed the multi-pulse network in the special case of $L = 1$ test pulses, which is not surprising because it was trained for this special case. Still, with 4 overlapping pulses, the multi- L network achieves an absolute error of only 4.0%.

4. CONCLUSION

In this work, we considered the classification of complex-valued time-domain radar pulses specified by a large labeled dataset. For this purpose, we designed a complex-valued ResNet with optimized parameters, including width, depth, kernel width, batch size, and learning rate. We also optimized the input dimension, necessitating either waveform truncation or noise-padding (as appropriate). Our training procedure used random delays, random noise waveforms, and a wide range of SNRs for robustness and to avoid overfitting. After fine-tuning, our network achieved a test error of 0.14% on single-pulse classification of asynchronous SI-DLE data, which is a 100x improvement over the previous state-of-the-art approach [5], which achieved 18.29%. When trained for multi-pulse classification, our network obtained an absolute error of 4.0% with 4 overlapping pulses. For future work, it would be interesting to investigate alternative approaches to multi-pulse classification, such as formulating it as a time-domain object detection problem.

5. REFERENCES

- [1] S. Haykin, “Cognitive radar: A way of the future,” *IEEE Signal Process. Mag.*, vol. 1, pp. 30–40, Jan. 2006.
- [2] J. Lunden and V. Koivunen, “Automatic radar waveform recognition,” *IEEE J. Sel. Topics Signal Process.*, vol. 1, pp. 124–136, May 2007.
- [3] B. Rigling and C. Roush, “ACF-Based classification of phase modulated waveforms,” in *Proc. IEEE Radar Conf.*, pp. 287–291, 2010.
- [4] A. Pavy and B. Rigling, “Phase modulated radar waveform classification using quantile one-class SVMs,” in *Proc. IEEE Radar Conf.*, pp. 745–750, 2015.
- [5] R. V. Chakravarthy, H. Liu, and A. M. Pavy, “Open-set radar waveform classification: Comparison of different features and classifiers,” in *Proc. IEEE Radar Conf.*, pp. 542–547, 2020.
- [6] K. He, X. Zhang, S. Ren, and J. Sun, “Deep residual learning for image recognition,” *arXiv:1512.03385*, 2015.
- [7] S. Xie, R. Girshick, P. Dollar, Z. Tu, and K. He, “Aggregated residual transformations for deep neural networks,” *arXiv:1161.05431v2*, 2017.
- [8] G. Huang, Z. Liu, L. Van Der Maaten, and K. Q. Weinberger, “Densely connected convolutional networks,” in *Proc. IEEE Conf. Comp. Vision Pattern Recog.*, pp. 4700–4708, 2017.
- [9] M. Wharton, E. T. Reehorst, and P. Schniter, “Compressive SAR image recovery and classification via CNNs,” in *Proc. Asilomar Conf. Signals Syst. Comput.*, pp. 1081–1085, 2019.
- [10] T. J. O’Shea, J. Corgan, and T. C. Clancy, “Convolutional radio modulation recognition networks,” in *Prof. Intl. Conf. Eng. Appl. Neural Netw.*, pp. 213–226, 2016.
- [11] C. Trabelsi, O. Bilaniuk, Y. Zhang, D. Serdyuk, S. Subramanian, J. F. Santos, S. Mehri, N. Rostamzadeh, Y. Bengio, and C. J. Pal, “Deep complex networks,” *arXiv:1705.09792*, 2017.
- [12] E. K. Cole, J. Y. Cheng, J. M. Pauly, and S. S. Vasanawala, “Analysis of deep complex-valued convolutional neural networks for MRI reconstruction,” *arXiv:2004.01738*, 2020.
- [13] E. Stevens, L. Antiga, and T. Viehmann, *Deep Learning with PyTorch*. Shelter Island, NY: Manning, 2020.
- [14] I. Goodfellow, Y. Bengio, and A. Courville, *Deep Learning*. MIT Press, 2016.